Organomineral nanocomposite carbon burial during Oceanic Anoxic Event 2

S. C. Löhr[1] and M. J. Kennedy[1]

[1]{Sprigg Geobiology Centre, School of Earth and Environmental Science, University of Adelaide, Adelaide 5005, Australia}

Correspondence to: S. C. Löhr (stefan.loehr@adelaide.edu.au)

Abstract

Organic carbon (OC) enrichment in sediments deposited during Oceanic Anoxic Events (OAEs) is commonly attributed to elevated productivity and marine anoxia. We find that OC enrichment in the late Cenomanian aged OAE2 at Demerara Rise was controlled by co-occurrence of anoxic bottom-water, sufficient productivity to saturate available mineral surfaces and variable deposition of high surface area detrital smectite clay. Redox indicators show consistently oxygen-depleted conditions, while a strong correlation between OC concentration and sediment mineral surface area (R^2=0.92) occurs across a range of TOC values from 9-33%. X-ray diffraction data indicates intercalation of OC in smectite interlayers while electron, synchrotron infrared and X-ray microscopy show an intimate association between clay minerals and OC, consistent with preservation of OC as organomineral nanocomposites and aggregates rather than discrete, µm-scale pelagic detritus. Since the consistent ratio between TOC and mineral surface area suggests that excess OC relative to surface area is lost, we propose that it is the varying supply of smectite that best explains variable organic enrichment against a backdrop of continuous anoxia, which is conducive to generally high TOC during OAE 2 at Demerara Rise. Smectitic clays are unique in their ability to form stable organomineral nanocomposites and aggregates that preserve organic matter, and are common weathering products of continental volcanic deposits. An increased flux of smectite coinciding with high carbon burial is consistent with evidence for widespread volcanism during OAE2, so that organomineral carbon burial may represent a potential feedback to volcanic degassing of CO_2.

1 Introduction

The geological record is punctuated by intervals of widespread organic carbon (OC) enrichment known as Oceanic Anoxic Events (OAEs) (Arthur and Sageman, 1994; Jenkyns, 2010; Schlanger and Jenkyns, 1976). Latest Cenomanian aged OAE2 (Cenomanian/Turonian boundary ≈ 93.9 Myr ago) is considered the best developed and most widespread OC enriched interval interpreted as resulting from an OAE as it shows evidence of deep-water anoxia as well as a general continuity of black shale deposition across Atlantic and Tethyan basins (Arthur et al., 1987). A positive $\delta^{13}C$ excursion in bulk organic matter (up to 7 ‰) and carbonates (2-3 ‰) implies global OC burial increased by 130% during this period (Arthur et al., 1988; Erbacher et al., 2005), and was accompanied by a selective extinction event that most severely affected benthic organisms and has been attributed to deep-water oxygen depletion (Kaiho and Hasegawa, 1994). OAE2 also coincides with greenhouse conditions including high atmospheric pCO_2 (Bice and Norris, 2002; van Bentum et al., 2012), low oxygen conditions in a warm ocean (Friedrich et al., 2012) and a period of intensified volcanism (Sinton and Duncan, 1997; Turgeon and Creaser, 2008) which may have triggered expansion of anoxia through release of hydrothermal fluids (Orth et al., 1993; Sinton and Duncan, 1997) and stimulation of primary productivity (Adams et al., 2010).

Organic enrichment in marine sediments during OAEs shows a complex mixture of influences (Arthur and Sageman, 1994; Kuypers et al., 2004), but is most commonly attributed to bottom-water anoxia and/or increased primary productivity (e.g. Arthur and Sageman, 1994; Mort et al., 2007). A basinwide tendency toward OC enrichment is modulated by local continental influences that dominate particular records (Beckmann et al., 2005) raising the fundamental question of whether additional mechanism are required for OC concentration. Continental effects may be indirectly expressed through oceanographic processes such as enhanced freshwater run-off causing stratification (Beckmann et al., 2005) and/or nutrient delivery (Pratt, 1984), however recent studies of modern and ancient continental margin sediments identify an additional influence via the OC preservation effects of detrital mineral surfaces (Keil and Cowie, 1999; Kennedy and Wagner, 2011; Mayer, 1994). This work showed that organic matter of marine origin is stabilized through association with terrestrially derived clay minerals, in particular high surface area smectitic clays. Mineral surface association stabilisation is particularly effective where it occurs in association with anoxia

because anoxia supports high dissolved OC, excludes bioturbators and reduces oxidant exposure time (Blair and Aller, 2012; Hedges et al., 1999; Keil and Cowie, 1999; Kennedy and Wagner, 2011).

The general importance of mineral surfaces is yet to be determined, but is pertinent because concentrations resulting from their effects have very different implications for the origin of organic rich rocks than purely oceanographic mechanisms. Reactive, high surface area detrital clay minerals such as smectite form in soils and by weathering of volcanic rocks (Chamley, 1989), so they represent a continental influence. However, since most smectite forms under sub-tropical, seasonally contrasted conditions and is subsequently eroded and transported to continental margins by rivers, this implies a spatially constrained distribution limited by zonal climate (Chamley, 1989). Thus, the potential influence of smectite on the basinal scale OC enrichment evident during OAE2 (Takashima et al., 2006) remains unclear.

Here we look at a deep marine section that is persistently oxygen-depleted through the OAE2 interval, yet shows large variation in TOC. We test whether variable OC enrichment is the result of fluctuating supply of detrital clays with a preservative effect on OC, combining characterization of bulk sediment properties with high resolution, electron microscope and synchrotron-based imaging of organic matter distribution and its association with clay minerals. We further consider potential mechanisms that could result in a basin-scale clay mineral influence on carbon burial.

2 Study Materials

A thick sequence (>80m) of organic rich sediments representative of the equatorial North Atlantic margin, including OAE2, were recovered during Ocean Drilling Program (ODP) Leg 207 at Demerara Rise. High hydrogen indices (mostly >500 mg HC/g OC), RockEval T_{max} <400^{o}C and the dominance of hopanes and steranes retaining their biological structural configurations suggest that the bulk of the organic matter (OM) in these sequences is marine in origin and thermally immature (Forster et al., 2004; Meyers et al., 2006), so that we expect the original OC-mineral associations established within the depositional environment to be retained (Kennedy et al., 2014). We collected and analysed a total of 120 samples at 10 cm spacing from ODP Sites 1258, 1260 and 1261, across the positive $\delta^{13}C$ excursion interpreted to mark the onset of OAE2 (Erbacher et al., 2005).

3 Methods

All samples for bulk analysis were ground in an agate mortar and pestle to pass through a 200 μm sieve. Subsamples for sediment mineral surface area (MSA) determination were shaken in 1M $CaCl_2$ for 1 hour, triple-rinsed in deionised water and oven-dried (110 °C for 48 hours). MSA measurements were determined using ethylene glycol monoethyl ether (EGME), following the 'free surface' procedure of Tiller and Smith (1990), using a factor of 3.2 to convert the mass of adsorbed EGME (mg) to mineral surface area (m^2), based on an assumption of monolayer coverage (Kennedy and Wagner, 2011). MSA was adjusted for $CaCO_3$ and OC content and is reported here as 'silicate MSA'. Six replicates of a suite of clay mineral standards obtained from the Clay Mineral Society and included in the same batch as the samples showed excellent reproducibility (SWy-2: 743 $m^2\ g^{-1}$ ± 0.52 %; STx-1b: 791 $m^2\ g^{-1}$ ± 0.29 %; IMt-2: 104 $m^2\ g^{-1}$ ± 2.57 %).

Total carbon was determined with a LECO Truespec CHN analyser. Inorganic C was determined using the pressure calcimeter method of Sherrod *et al.* (2002). Organic C was calculated as the difference between total C and inorganic C, and is reported on a carbonate-free basis to account for the effects of carbonate dilution. Major and trace element chemistry of Site 1261 samples was determined using standard X-ray fluorescence methods (Philips PW 1480 XRF) on fused disks and pressed pellets, respectively.

Sample mineralogy was determined by X-ray diffraction (Bruker D8 Advance X-ray diffractometer with a Cu source) on micronised powders (incl. 10% ZnO internal standard). Clay mineralogy of the samples was determined on Ca-saturated oriented preparations of the <2 μm fraction (air dried and after treatment with ethylene glycol). The < 2 μm fraction was obtained by centrifugation after carbonate removal with 1M sodium acetate buffer at pH 5 and 90 ^oC, OM removal with NaOCl at pH 9.5 and 90 ^oC, and ultrasonic dispersal. To test for OM intercalation in the smectite interlayer the < 2 μm fraction of selected samples was also obtained without chemically pretreating the samples. These samples were air-dried and analysed as above. They were then reanalysed after heating for 24 hours at temperatures of 105, 200, 300 and 400 ^oC, following the procedure of Theng et al. (1986).

The micro to nano-scale distribution and association of clay minerals and OC was determined on a) ion-polished samples by scanning electron microscopy (SEM) backscatter electron (BSE) imaging and energy dispersive X-ray analysis, and b) cryomicrotomed, 300 nm thick ultrathinsections by imaging these at the Infrared Microscope (FTIR) beamline of the

Australian Synchrotron and the Scanning Transmission X-ray Microscope (STXM) beamline of the Swiss Light Source. A more detailed description of the electron and synchrotron based imaging methods, including sample preparation, is given in Appendices A to D.

4 Results and Discussion

Our results identify a strong, positive relationship between sediment MSA and TOC at all three sites (Figs. 1 and 2), both prior to and within the OAE2 interval, where MSA accounts for 87% to 92% of variation in TOC content of the samples across a range in TOC from 8.9-33.4% of the non-carbonate portion of the sediment. Since we present data for the carbonate-free fraction, we can discount the possibility that the correlation between MSA and TOC is due to changes in the relative abundance of carbonate. Quartz and biogenic opal are other potentially abundant sediment components, but the absence of a negative correlation between the Al-normalised concentrations of OC and Si (Fig. 4) demonstrates that varying dilution by quartz or biogenic silica is not a significant influence on sediment TOC. These finely laminated sediments were deposited from suspension as pelagic or hemipelagic deposits and do not show evidence of current winnowing or concentration such as erosional scours or traction. We thus attribute abrupt changes in MSA to changes in supply of high MSA phases such as smectite clay from the terrestrial source region. MSA tracks abrupt, high-amplitude shifts of TOC (up to 17%) between successive samples where mineralogy of the sediment reflects a primary depositional relation (Fig. 1). Further, trends in MSA do not lead or lag TOC as might be expected if changes in these indices were indirectly related through a shared environmental control; the proportional sample to sample shifts strongly support a direct mechanistic relationship between OC and MSA, implying preservation of sub-micron scale OC closely associated with clay mineral surfaces, which provide the bulk of sediment MSA (Keil and Mayer, 2014; Kennedy and Wagner, 2011; Ransom et al., 1998). This is consistent with the OC preservation effects of detrital (soil derived) mineral surfaces in modern marine sediments (Blair and Aller, 2012; Keil and Mayer, 2014).

Sediments in modern continental margin settings show two distinct components of OC; discrete organic particles >1μm and a mineral associated component that cannot be separated by physical means (Keil et al., 1994b). The mineral associated phase is considerably more refractory (Keil et al., 1994a) and remains relatively constant through the sediment profile. Quantification of the discrete OC phase (Keil et al., 1994b) and comparison of OC to MSA ratios (Mayer, 1994) show that while discrete OM (particles) is commonly dominant at the

sediment-water interface, it generally comprises < 10% of OC by 30 cm of the sediment profile. The refractory properties of the mineral associated fraction make it a more likely component to survive the seafloor diagenetic reactions and enter the geologic record. While a correlation between MSA and TOC has been documented in the few examples of black shale where this relation has been studied (Kennedy and Wagner, 2011; Kennedy et al., 2014; 2002), previous work has relied mainly on bulk sample characterization rather than direct assessment of clay-organic associations.

Direct imaging of the distribution of OC and its association with mineral surfaces provides an ultimate test to discriminate this sub-µm organo-mineral style of preservation from preservation of the discrete, micron-sized organic detritus of pelagic origin that is typically considered to constitute the organic fraction (Tyson, 1995). SEM BSE imaging of ion-polished samples demonstrates that OC is widely distributed through the sediment, where it is typically associated with and coats clay minerals, forming organoclay aggregates (Fig. 5), as in modern sediments (Blair and Aller, 2012; Keil and Mayer, 2014). Although individual aggregates can have the appearance of discrete OM particles (Fig. 5A), energy dispersive X-ray analysis (Fig. 5D) and closer inspection at higher magnifications (Fig. 5B+C) reveals the composite clay-organic nature of these zones. Synchrotron Fourier Transform Infrared (FTIR) and Scanning Transmission X-ray (STXM) microspectroscopy of multiple cryomicrotomed ultrathinsections of seven samples, selected across a range of TOC and MSA values, independently confirms that OC and clay minerals have overlapping distributions and are disseminated throughout the sediment where they are spatially associated (Fig. 6).

A limitation of the small, µm-scale field of view of the high resolution images is that establishing that any given image is representative of the primary form of OC is problematic, so that we offer this type of data only as a proof of concept while relying on the bulk rock relations (MSA-TOC) to identify the extent of the organo-clay relationship. Thus, our assessment of the relative abundance of clay-associated vs discrete OM is based on the strong bulk sample relationship between MSA and TOC, which implies that the great majority of OM is associated with clay minerals, and that the OM is sufficiently small to meaningfully interact and associate with clays (Keil and Mayer, 2014; Kennedy et al., 2014; Mayer, 1994). Not only is discrete OM detritus too large to meaningfully interact with the clay mineral matrix, if particulate OC from pelagic sources (and unrelated to mineral surface associated OC) where an important contributor to some of the samples these would plot above the

regression evident in Figure 2 (high TOC with limited surface area) indicating the presence of OC that was independent and unrelated to the TOC-MSA scaling relationship. Yet samples with high TOC relative to MSA are not apparent in our dataset, and our high resolution images show an intimate, sub-µm scale association between clays and OM. Thus, we argue that OC is preserved mainly as sub-µm organic matter in close association with clays, rather than as discrete, µm-scale organic particles. These findings strongly support a mechanistic link between OC and clays where the great majority of OC is quantitatively associated with and stabilized by clay mineral surfaces.

Within this context, what is the impact of oxygen availability and productivity on OC enrichment at Demerara Rise? Measured concentrations of sulfur-bound isorenieratane and chlorobactane imply that the photic zone was periodically sulfidic (euxinic) both before and during OAE2 (van Bentum et al., 2009), however the scattered occurrence of inoceramids (Jiménez Berrocoso et al., 2008) as well as a low abundance and diversity of benthic foraminifera (Friedrich et al., 2006) and fecal pellets and fossils of nektonic fauna (Nederbragt et al., 2007) show that water column euxinia was intermittent. Undisrupted lamination and elevated concentrations of redox sensitive trace metals (Hetzel et al., 2009) suggest that sea floor anoxic conditions at Demerara Rise both preceded and postdated the interval identified as OAE2. Consistent with these findings, our trace element data suggests continuously oxygen-depleted bottom-waters at Site 1261 (Fig. 4). Fluctuating P/Al ratios and the intermittent presence of apatite in the pre-OAE2 section imply redox conditions alternating between a) anoxic, non-sulfidic conditions permitting apatite precipitation and preservation and b) sulfidic conditions which resulted in removal of P released during microbial degradation of OC (Hetzel et al., 2009; März et al., 2008; Tribovillard et al., 2006), whereas persistently lower P concentrations during the OAE2 interval (Fig. 4) suggest more consistently sulfidic conditions and efficient P recycling (März et al., 2008). This is supported by short intervals of elevated Al-normalised Mo and Ni concentrations prior to OAE2, which correspond to low P intervals, and are indicative of periodically sulfidic conditions, whereas a positive correlation between Zn and V, as well as Mo and Ni, within the OAE2 interval is indicative of more persistently sulfidic conditions (Hetzel et al., 2009; Jiménez Berrocoso et al., 2008; Tribovillard et al., 2006). While the continuously oxygen-deficient conditions interpreted on the basis of these results are generally conducive to enhanced OC preservation, all proxy records for oxygen variability fail to reproduce the higher order sample to sample TOC variability (Fig. 4). This is unsurprising because minor variations in already oxygen-

depleted conditions are by themselves unlikely to be expressed as differences in TOC as great as the observed variation from 9-26% in adjacent samples (Tyson, 2005). Fluctuating productivity, on the other hand, is a potential explanation for variable OC enrichment such as observed here (Kuypers et al., 2004). The strongly reducing depositional environment at Demerara Rise precludes quantitative reconstruction of palaeoproductivity trends using proxies such as Ba (Hetzel et al., 2009). However, the strong association and constant ratio between TOC and MSA in our dataset, and the absence of high or low TOC relative to MSA in particular, demonstrates that the pattern of OC enrichment is not a function of variable OC inputs. While productivity sufficient to saturate available surfaces and maintain anoxic conditions through respiration is an essential requirement, the bulk relationship also necessitates breakdown of μm-scale pelagic organic detritus, which likely represents a source of OC for mineral association within the sediment, and loss of OC in excess of the preservative capacity of the sediment. This is consistent with the downcore loss of OC during early diagenesis observed in modern marine settings (Mayer, 1994) and the low abundance of discrete, μm size organic detritus of pelagic origin in Demerara sediments. Finally, mineral surface association slows but does not stop OC degradation in oxic settings, whereas persistent oxygen depletion increases the preservative capacity of the sediments through lower oxidant concentrations, limited redox oscillations, exclusion of benthic infauna and higher porewater OC, enabling higher OC loadings per unit MSA (Blair and Aller, 2012; Burdige, 2007; Hedges and Keil, 1995; Hedges et al., 1999; Keil and Cowie, 1999). We thus propose that a clay mineral preservative effect combined with persistently oxygen-depleted conditions best explains the variable but high TOC at Demerara Rise.

The preservative effect on OC afforded by mineral surfaces has been attributed to physicochemical stabilization by direct sorption of OC to mineral surfaces (Bennett et al., 2012; Curry et al., 2007) and exclusion of microbial decomposers and their exoenzymes by physical encapsulation of labile organic matter (Keil et al., 1994a; Mayer, 1994), but the exact preservative mechanisms remain poorly understood. Given the physical association of OC directly on clay surfaces and the compartmentalized architecture of organoclay aggregates (Fig. 5), it is likely that both encapsulation and sorptive stabilisation contribute to the preservation of OC in organomineral aggregates (Bennett et al., 2012; Curry et al., 2007; Keil and Mayer, 2014). The MSAs measured in this study lie within the range of surface area values characteristic of smectite clay (~750 m^2 g^{-1}; Środoń, 2009), and smectite interlayer surfaces in particular, implying that these interlayer sites also play an important role in the

preservation of nanometer scale OC. Smectite clays have substantially greater surface area than other common sedimentary minerals because smectite layers consist of an octahedral sheet sandwiched between two tetrahedral sheets, and these fundamental units stack together to form an interlayer between them. The interlayer is expandable so that interlayer sites are accessible to polar and non-polar organic molecules, ions and water (Alimova et al., 2009; Theng et al., 1986; Williams et al., 2005), with interlayer surface area contributing the bulk of smectite total surface area. The preservative effect on OC by smectite has thus been hypothesized to be the result of incorporation of molecular scale organic compounds in the smectite interlayer space (Kennedy et al., 2002; Theng et al., 1986), forming refractory organo-mineral nanocomposites that protect OC molecules from degradation. This is supported by our results. X-ray diffraction of clay separates identifies the dominance of smectite clays in Demerara sediments (Fig. E2), confirming that MSA variation is due to varying smectite content, and clearly identifies the organomineral nanocomposite nature of this material (Fig. 7), where a component of OM is preserved as molecular scale OM intercalated within the smectite interlayer. Independent palynologic analysis (Summerhayes, 1981) of Demerara Rise sediments is consistent with our evidence for organomineral intercalation and mineral associated OC preservation. These analyses rely on the dissolution of the silicate fraction to concentrate OM and show that > 90% of Demerara Rise OM is amorphous and of unrecognizable origin, likely comprising the acid-insoluble residue of previously mineral-associated organic material. Consistent with our interpretation, recognizable organic detritus does not constitute a quantitatively significant component of sediment TOC (Summerhayes, 1981).

The x-axis intercepts of the Demerara Rise MSA/TOC regressions (Figure 2) are offset from zero (≈200 m^2/g). This is similar to offsets of ≈260 m^2/g and ≈290 m^2/g for the anoxic/suboxic and the oxic facies, respectively, of OAE3 at ODP Site 959 (Deep Ivorian Basin; Kennedy and Wagner, 2011) and an offset of ≈60 m^2/g for the Cretaceous Pierre Shale (Kennedy et al., 2002). This x-intercept offset implies MSA that did not acquire OM or subsequently lost OM. It has previously been interpreted to reflect loss of a more readily oxidised fraction of OM that was associated with external clay mineral surfaces and edges (which can exceed 200 m^2/g in smectitic sediments) whereas OM preserved within the smectite interlayer is considered to be more refractory (Kennedy and Wagner, 2011; Kennedy et al., 2014). However, SEM observations of organoclay aggregates from Demerara Rise identify a component of OM associated with external clay surfaces, encapsulated within

organoclay aggregates. The observed offsets may be the product of lower OM concentrations in the outermost zone of these aggregates. OM encapsulated by and sorbed to clays in aggregate interiors is progressively better protected relative to OM initially present closer to the aggregate exterior (Keil and Mayer, 2014), as also documented for soil organomineral aggregates (Kinyangi et al., 2006).

Finally, the slope of the MSA to TOC regression has been shown to vary as a function of the depositional environment, sediment diagenesis, and oxic versus anoxic sediments (Blair and Aller, 2012; Kennedy and Wagner, 2011). While TOC generally correlates with MSA in modern continental margin sediments, the highest OM loadings per unit MSA (slope) are found in sediments from high productivity and/or oxygen depleted settings whereas the lowest loadings are typical of sediments from higher energy settings or deep-sea deposits that are subject to long oxidant exposure times (Blair and Aller, 2012). Similar differences are apparent in ancient sediments, with higher OM loadings recorded in samples from anoxic facies (0.7 mg OC/m^2) compared to oxic and suboxic facies (0.4 mg OC/m^2) at ODP Site 959 (Kennedy and Wagner, 2011). While the ODP 959 and Demerara Rise datasets largely overlap, the slope of the MSA to TOC regression at Demerara Rise sites ranges between 0.44 mg OC/m^2 (Site 1258) and 0.52 mg OC/m^2 (Site 1260), somewhat lower than the laminated, anoxic facies at Site 959 but greater than the oxic to suboxic facies at Site 959. Although this might indicate greater oxidant exposure at Demerara Rise relative to Site 959, comparison to modern sediments show that OM loading ratios are equally reduced in relatively higher energy, lower productivity, or lower sedimentation rate settings.

5 Conclusions

The organic carbon deposits defining OAE2 are widely considered a response to increased productivity and reduced oxidant concentration in seawater, likely triggered by volcanism. Our results show that high but variable OC enrichment at Demerara Rise, including the OAE2 interval, is due to the intersection of consistently oxygen depleted conditions and variable deposition of detrital smectite clay capable of forming refractory organomineral nanocomposites and aggregates, representing a continental influence. But can the smectite influence on OC burial identified at Demerara Rise potentially explain anomalous OC enrichment during OAE2 at other geographically distant locations, given that smectite formation in soils is spatially constrained by zonal climate (Chamley, 1989)?

Smectite is also a major weathering product of continental volcanic deposits. Volcanism can lead to regional or even basinal scale increases in smectite concentration because of transport of this finest clay fraction over 100s or even 1000s of km along basin margins (Chamley, 1989). Sr, Os, Nd and S isotope anomalies measured across the C isotope excursion that defines OAE2 show an increase in mantle derived fluids at geographically distant locations (Adams et al., 2010; Jones and Jenkyns, 2001; Martin et al., 2012; Turgeon and Creaser, 2008). This is closely timed with the emplacement of the Caribbean and Madagascar large igneous provinces (Kerr, 1998; Sinton and Duncan, 1997) and the production and geographic dispersal of easily weathered volcanic materials from these sources (Kuroda et al., 2007). Thus, a pulse of subaqueous (Turgeon and Creaser, 2008) and subaerial (Kuroda et al., 2007) volcanism coinciding with OAE2 may not only have stimulated marine productivity (Adams et al., 2010) and contributed to the geographic expansion of anoxic conditions (Sinton and Duncan, 1997), increased subaerial weathering of volcanic material may also have amplified the flux of detrital smectite to continental margin settings (Nadeau and Reynolds, 1981), producing conditions conducive to anomalous accumulation of OC during OAE2. If confirmed, this would represent a previously unrecognized negative feedback mechanism that balances CO_2 produced during widespread phases of volcanic with removal of CO_2 through enhanced sequestration of organic matter as organomineral nanocomposites.

Appendix A: SEM analyses

Organic matter morphology, distribution and mineral association was determined at mm to sub-µm scales using a FEI Quanta 450 environmental scanning electron microscope system equipped with a backscattered electron (BSE) detector and energy dispersive X-ray (EDAX) analyser. Prior to imaging samples were fixed onto SEM stubs with the imaged surface prepared perpendicular to bedding. Samples were gently dry ground until flat, cleaned with compressed nitrogen, ion milled until polished (Fischione 1010 Ar Ion Mill system) and coated with 5 nm Pt.

Appendix B: Synchrotron imaging sample preparation

Transmission imaging requires preparation of intact ultrathinsections. A cryomicrotoming approach was utilised in order to avoid embedding samples in carbon-based resin (Lehmann et al., 2008). Intact shale subsamples were mounted onto microtome pins and saturated in ultrapure water overnight. Excess water was drained on a filter paper after which samples

were plunge-frozen in liquid nitrogen. Thin sections (300 nm thickness) were cryomicrotomed (Leica Ultracut S) across the shale bedding plane at -80°C using a diamond knife at a cutting speed of 2.5 mm sec^{-1}. Sections were then transferred and pressed onto C-free Cu grids (200 mesh with SiO membrane, No. 53002, Ladd Research, Williston, VT) before being air-dried.

Appendix C: IR data collection and analysis

Fourier Transform Infrared (FTIR) spectra of the cryomicrotomed ultrathinsections were collected in transmission mode at the Infrared microspectroscopy beamline at the Australian Synchrotron. The beamline is equipped with a Bruker Hyperion 2000 microscope with Vertex V80v FTIR spectrometer, and a narrow band, high sensitivity liquid nitrogen cooled Mercury Cadmium Telluride detector. Spectral maps of the thin sections were recorded with a 5-µm aperture size and a step size of 5 µm, a spectral range of 3900 – 700 cm^{-1} and a spectral interval of 4 cm^{-1}. Each spectrum was composed of 64 scans added before Fourier transformation. All spectra were corrected for adsorption from the grid membrane by normalising to the spectrum of an empty region of the grid. FTIR data was processed using Bruker OPUS 6.5 software (Bruker Optics, Billerica, Massachusetts, USA). Spectral maps were created after cropping to a spectral region of 3800 to 850 cm^{-1} and automatic baseline correction (concave rubber-band method, 10 iterations, 64 baseline points). Maps were created for maximum peak heights in the following ranges: 2935 to 2920 cm^{-1} and 1060 to 1020 cm^{-1}. A peak position at 2935 to 2920 cm^{-1} corresponds to C–H stretching vibrations of aliphatic C (Haberhauer et al., 1998; Lehmann et al., 2007) and at 1060 to 1020 cm^{-1} to the principal SiO stretching band of smectite, illite or interstratified illite-smectite (Russell and Fraser, 1994).

Appendix D: STXM data collection and analysis

Scanning Transmission X-ray Microscope (STXM) maps of nanoscale C distribution were collected at the PolLux beamline of the Swiss Light Source, which is situated on a bend-magnet type synchrotron beamline that provides a linearly polarized X-ray beam with a photon energy range between approximately 250 eV and 1600 eV. Detailed descriptions of the beam-line and applications of the STXM technique are published elsewhere (Raabe et al., 2008). Briefly, while a monochromatic X-ray beam is focused on the sample by a Fresnel zone plate (25 nm outer zone width), the sample is scanned through the beam and the transmitted intensity yields the 2D image with a focus spot size of about 25 nm (Raabe et al.,

2008; Watts and Ade, 2012). Element-specific contrast stems from differing X-ray absorption at energies below and above the element-specific absorption edge, which is approximately 300 eV at the C K-edge (Watts and Ade, 2012). The ratio of images taken below and above the absorption edge then shows the distribution and concentration of the element of interest. Accordingly, each ultrathinsection was scanned at 280 and 320 eV using a spot resolution of 25 nm, a step size of 600 nm and a dwell time of 5 ms. Selected areas where then scanned at higher resolution, typically with a step size of 50 nm, all other parameters remaining unchanged.

Appendix E: Supplementary Figures

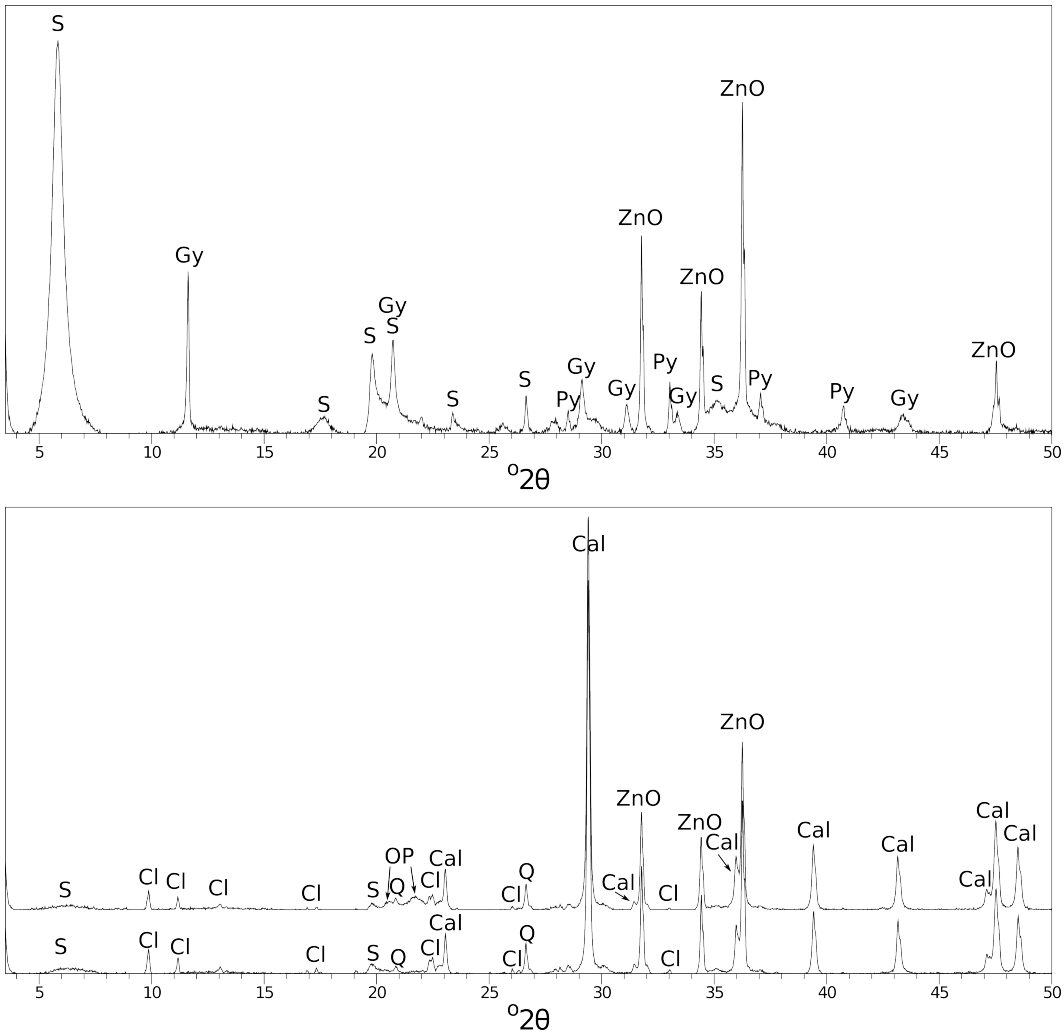

Figure E1. X-ray diffractograms of an altered ash layer sample (upper panel; Sample 1261/A/48R/5/30-31) and two typical non-ash layer samples (lower panel; Samples 1258/A/43R/2/65-66 and 1258/A/43R/2/85-86). The samples showing elevated MSA with relatively low TOC at Sites 1260 and 1261 are altered volcanic ash (bentonite). These samples are composed mainly of smectite clay and lack other detrital or biogenic phases typical of other Demerara Rise sediments. Diagenetic smectite forms after burial by *in situ* alteration of volcanic glass in ash beds, and does not exhibit the MSA – OC associations of detrital smectite because the diagenetic smectite forms after the sediment is decoupled from OC-sources in the water column or pore water. S=smectite, Gy=gypsum, Py=pyrite, Cl=clinoptilolite, OP=opal CT, Q=quartz, Cal=calcite, ZnO=zinc oxide internal standard.

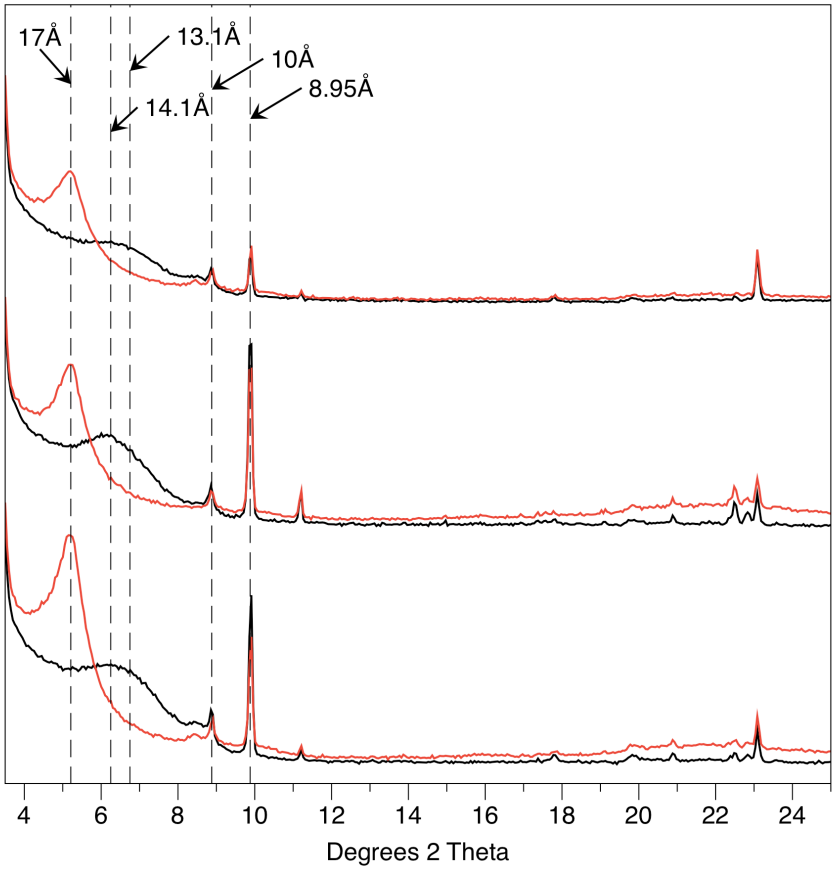

Figure E2. Air dried (black) and ethylene glycol treated (red) X-ray diffractograms of the <5 µm fraction show a predominance of smectite (expands from 13-14Å to 17Å after glycolation) and smaller amounts of discrete illite (10Å) in Demerara Rise samples. Clinoptilolite, a diagenetic zeolite, is also present in this size fraction in many samples (8.95 Å). Top: 1261/A/49R/1/95-96; Middle: 1261/A/48R/5/130-131; Bottom: 1261/A/48R/4/65-66.

Acknowledgements

We thank the Australian Research Council for financial support (ARC Discovery Project DP110103367 to MJK), and we acknowledge travel funding (AS/IA122/5177) provided by the International Synchrotron Access Program (ISAP) managed by the Australian Synchrotron and funded by the Australian Government. We thank J. Brugger and B. Etschmann for their help with FTIR and STXM experiments, and staff at Adelaide Microscopy for assistance with sample preparation. FTIR experiments were undertaken at the Australian Synchrotron. STXM experiments were performed on the X07DA (PolLux) beamline of the Swiss Light Source. This research used samples and data provided by the

Ocean Drilling Program (ODP). ODP is sponsored by the U.S. National Science Foundation (NSF) and participating countries under management of Joint Oceanographic Institutions (JOI), Inc.

References

Adams, D. D., Hurtgen, M. T. and Sageman, B. B.: Volcanic triggering of a biogeochemical cascade during Oceanic Anoxic Event 2, Nat Geosci, 3(3), 201–204, doi:10.1038/NGEO743, 2010.

Alimova, A., Katz, A., Steiner, N., Rudolph, E., Wei, H., Steiner, J. C. and Gottlieb, P.: Bacteria-Clay Interaction: Structural Changes in Smectite Induced During Biofilm Formation, Clays Clay Miner, 57(2), 205–212, doi:10.1346/CCMN.2009.0570207, 2009.

Arthur, M. A. and Sageman, B. B.: Marine Black Shales - Depositional Mechanisms and Environments of Ancient Deposits, Annu. Rev. Earth Planet. Sci., 22, 499–551, 1994.

Arthur, M. A., Dean, W. E. and Pratt, L. M.: Geochemical and Climatic Effects of Increased Marine Organic-Carbon Burial at the Cenomanian Turonian Boundary, Nature, 335(6192), 714–717, 1988.

Arthur, M. A., Schlanger, S. O. and Jenkyns, H. C.: The Cenomanian-Turonian Oceanic Anoxic Event, II. Palaeoceanographic controls on organic-matter production and preservation, Geological Society Special Publications, 26, 401–420, 1987.

Beckmann, B., Flögel, S., Hofmann, P., Schulz, M. and Wagner, T.: Orbital forcing of Cretaceous river discharge in tropical Africa and ocean response, Nature, 437(7056), 241–244, doi:10.1038/nature03976, 2005.

Bennett, R. H., Hulbert, M. H., Curry, K. J., Curry, A. and Douglas, J.: Organic matter sequestered in potential energy fields predicted by 3-D clay microstructure model: Direct observations of organo-clay micro- and nanofabric, Marine Geology, 315-318, 108–114, 2012.

Bice, K. and Norris, R.: Possible atmospheric CO2 extremes of the Middle Cretaceous (late Albian-Turonian), Paleoceanography, 17(4), –, doi:10.1029/2002PA000778, 2002.

Blair, N. E. and Aller, R. C.: The Fate of Terrestrial Organic Carbon in the Marine Environment, Annual Review of Marine Science, 4, 401–423, doi:10.1146/annurev-marine-120709-142717, 2012.

Burdige, D. J.: Preservation of Organic Matter in Marine Sediments: Controls, Mechanisms, and an Imbalance in Sediment Organic Carbon Budgets? Chem. Rev., 107(2), 467–485, doi:10.1021/cr050347q, 2007.

Chamley, H.: Clay Sedimentology, Springer Verlag, Berlin. 1989.

Curry, K. J., Bennett, R. H., Mayer, L. M., Curry, A., Abril, M., Biesiot, P. M. and Hulbert, M. H.: Direct visualization of clay microfabric signatures driving organic matter preservation in fine-grained sediment, Geochim. Cosmochim. Acta, 71(7), 1709–1720,

doi:10.1016/j.gca.2007.01.009, 2007.

Erbacher, J., Friedrich, O., Wilson, P., Birch, H. and Mutterlose, J.: Stable organic carbon isotope stratigraphy across Oceanic Anoxic Event 2 of Demerara Rise, western tropical Atlantic, Geochem Geophy Geosy, 6(6), Q06010, doi:10.1029/2004GC000850, 2005.

Forster, A., Sturt, H., Meyers, P. A.Leg 207 Shipboard Scientific Party: Molecular biogeochemistry of Cretaceous Black Shales from the Demerara Rise: Preliminary Shipboard Results from Sites 1257 and 1258, Leg 207, in Proceedings of the Ocean Drilling Program, Initial Reports, vol. 207, edited by J. Erbacher, D. C. Mosher, and M. J. Malone. 2004.

Friedrich, O., Erbacher, J. and Mutterlose, J.: Paleoenvironmental changes across the Cenomanian/Turonian Boundary Event (Oceanic Anoxic Event 2) as indicated by benthic foraminifera from the Demerara Rise (ODP Leg 207), Revue de Micropaléontologie, 49, 121–139, 2006.

Friedrich, O., Norris, R. D. and Erbacher, J.: Evolution of middle to Late Cretaceous oceans-A 55 m.y. record of Earth's temperature and carbon cycle, Geology, 40(2), 107–110, doi:10.1130/G32701.1, 2012.

Haberhauer, G., Rafferty, B., Strebl, F. and Gerzabek, M.: Comparison of the composition of forest soil litter derived from three different sites at various decompositional stages using FTIR spectroscopy, Geoderma, 83, 331–342, 1998.

Hedges, J. and Keil, R. G.: Sedimentary Organic-Matter Preservation - an Assessment and Speculative Synthesis, Marine Chemistry, 49, 81–115, 1995.

Hedges, J., Hu, F., Devol, A., Hartnett, H., Tsamakis, E. and Keil, R. G.: Sedimentary organic matter preservation: A test for selective degradation under oxic conditions, Am. J. Sci., 299(7-9), 529–555, 1999.

Hetzel, A., Boettcher, M. E., Wortmann, U. G. and Brumsack, H.-J.: Paleo-redox conditions during OAE 2 reflected in Demerara Rise sediment geochemistry (ODP Leg 207), Palaeogeogr. Palaeoclimatol. Palaeoecol., 273, 302–328, doi:10.1016/j.palaeo.2008.11.005, 2009.

Jenkyns, H. C.: Geochemistry of oceanic anoxic events, Geochem Geophy Geosy, 11(3), doi:10.1029/2009GC002788, 2010.

Jiménez Berrocoso, A., MacLeod, K. G., Calvert, S. E. and Elorza, J.: Bottom water anoxia, inoceramid colonization, and benthopelagic coupling during black shale deposition on Demerara Rise (Late Cretaceous western tropical North Atlantic), Paleoceanography, 23(3), –, doi:10.1029/2007PA001545, 2008.

Jones, C. and Jenkyns, H.: Seawater strontium isotopes, oceanic anoxic events, and seafloor hydrothermal activity in the Jurassic and Cretaceous, Am. J. Sci., 301(2), 112–149, 2001.

Kaiho, K. and Hasegawa, T.: End-Cenomanian Benthic Foraminiferal Extinctions and Oceanic Dysoxic Events in the Northwestern Pacific-Ocean, Palaeogeogr. Palaeoclimatol. Palaeoecol., 111, 29–43, 1994.

Keil, R. G. and Cowie, G. L.: Organic matter preservation through the oxygen-deficient zone of the NE Arabian Sea as discerned by organic carbon:mineral surface area ratios, Marine Geology, 161(1), 13–22, doi:10.1016/S0025-3227(99)00052-3, 1999.

Keil, R. G. and Mayer, L. M.: Mineral Matrices and Organic Matter, in Treatise on Geochemistry, pp. 337–359, Elsevier. 2014.

Keil, R. G., Montlucon, D. B., Prahl, F. G. and Hedges, J.: Sorptive Preservation of Labile Organic-Matter in Marine-Sediments, Nature, 370(6490), 549–552, 1994a.

Keil, R. G., Tsamakis, E., Fuh, C. B., Giddings, J. C. and Hedges, J.: Mineralogical and textural controls on the organic composition of coastal marine sediments: Hydrodynamic separation using SPLITT-fractionation, Geochim. Cosmochim. Acta, 58(2), 879–893, 1994b.

Kennedy, M. J. and Wagner, T.: Clay mineral continental amplifier for marine carbon sequestration in a greenhouse ocean, Proc. Natl. Acad. Sci. USA, 108(24), 9776–9781, doi:10.1073/pnas.1018670108, 2011.

Kennedy, M. J., Löhr, S. C., Fraser, S. A. and Baruch, E. T.: Direct evidence for organic carbon preservation as clay-organic nanocomposites in a Devonian black shale; from deposition to diagenesis, Earth Planet. Sci. Lett., 388, 59–70, doi:10.1016/j.epsl.2013.11.044, 2014.

Kennedy, M. J., Pevear, D. and Hill, R.: Mineral Surface Control of Organic Carbon in Black Shale, Science, 295(5555), 657–660, doi:10.1126/science.1066611, 2002.

Kerr, A. C.: Oceanic plateau formation: a cause of mass extinction and black shale deposition around the Cenomanian-Turonian boundary? J Geol Soc London, 155, 619–626, 1998.

Kinyangi, J., Solomon, D., Liang, B., Lerotic, M., Wirick, S. and Lehmann, J.: Nanoscale biogeocomplexity of the organomineral assemblage in soil: Application of STXM microscopy and C 1s-NEXAFS spectroscopy, Soil Sci Soc Am J, 70(5), 1708–1718, doi:10.2136/sssaj2005.0351, 2006.

Kuroda, J., Ogawa, N. O., Tanimizu, M., Coffin, M. F., Tokuyama, H., Kitazato, H. and Ohkouchi, N.: Contemporaneous massive subaerial volcanism and late cretaceous Oceanic Anoxic Event 2, Earth Planet. Sci. Lett., 256, 211–223, doi:10.1016/j.epsl.2007.01.027, 2007.

Kuypers, M. M. M., Lourens, L. J., Rijpstra, W., Pancost, R., Nijenhuis, I. A. and Sinninghe Damsté, J. S.: Orbital forcing of organic carbon burial in the proto-North Atlantic during oceanic anoxic event 2, Earth Planet. Sci. Lett., 228, 465–482, doi:10.1016/j.epsl.2004.09.037, 2004.

Lehmann, J., Kinyangi, J. and Solomon, D.: Organic matter stabilization in soil microaggregates: implications from spatial heterogeneity of organic carbon contents and carbon forms, Biogeochemistry, 85(1), 45–57, doi:10.1007/s10533-007-9105-3, 2007.

Lehmann, J., Solomon, D., Kinyangi, J., Dathe, L., Wirick, S. and Jacobsen, C.: Spatial complexity of soil organic matter forms at nanometre scales, Nat Geosci, 1(4), 238–242, doi:10.1038/ngeo155, 2008.

Martin, E. E., MacLeod, K. G., Jiménez Berrocoso, A. and Bourbon, E.: Water mass circulation on Demerara Rise during the Late Cretaceous based on Nd isotopes, Earth Planet. Sci. Lett., 327-328(C), 111–120, doi:10.1016/j.epsl.2012.01.037, 2012.

Mayer, L. M.: Surface-Area Control of Organic-Carbon Accumulation in Continental-Shelf Sediments, Geochim. Cosmochim. Acta, 58(4), 1271–1284, 1994.

März, C., Poulton, S. W., Beckmann, B., Kuester, K., Wagner, T. and Kasten, S.: Redox sensitivity of P cycling during marine black shale formation: Dynamics of sulfidic and anoxic, non-sulfidic bottom waters, Geochim. Cosmochim. Acta, 72(15), 3703–3717, doi:10.1016/j.gca.2008.04.025, 2008.

Meyers, P. A., Bernasconi, S. M. and Forster, A.: Origins and accumulation of organic matter in expanded Albian to Santonian black shale sequences on the Demerara Rise, South American margin, Organic Geochemistry, 37(12), 1816–1830, doi:10.1016/j.orggeochem.2006.08.009, 2006.

Mort, H. P., Jacquat, O., Adatte, T., Steinmann, P., Foellmi, K., Matera, V., Berner, Z. and Stueben, D.: The Cenomanian/Turonian anoxic event at the Bonarelli level in Italy and Spain: enhanced productivity and/or better preservation? Cretaceous Res, 28(4), 597–612, doi:10.1016/j.cretres.2006.09.003, 2007.

Nadeau, P. H. and Reynolds, R. C.: Volcanic components in pelitic sediments, Nature, 294(5836), 72–74, doi:10.1038/294072a0, 1981.

Nederbragt, A. J., Thurow, J. and Pearce, R.: Sediment composition and cyclicity in the mid-Cretaceous at Demerara Rise, ODP Leg 207, in *Proc. ODP, Sci. Results,* 207, vol. 207, edited by D. C. Mosher, J. Erbacher, M. J. Malone, and R. E. Garrison, pp. 1–31, Ocean Drilling Program, College Station TX. 2007.

Orth, C. J., Attrep, M., Quintana, L., Elder, W., Kauffman, E., Diner, R. and Villamil, T.: Elemental Abundance Anomalies in the Late Cenomanian Extinction Interval - a Search for the Source(S), Earth Planet. Sci. Lett., 117, 189–204, 1993.

Pratt, L. M.: Influence of paleoenvironmental factors on preservation of organic matter in Middle Cretaceous Greenhorn formation, Pueblo Colorado, Am. Assoc. Pet. Geol., Bull.; (United States), 68:9, 1146–1159, 1984.

Raabe, J., Tzvetkov, G., Flechsig, U., Boege, M., Jaggi, A., Sarafimov, B., Vernooij, M. G. C., Huthwelker, T., Ade, H., Kilcoyne, D., Tyliszczak, T., Fink, R. H. and Quitmann, C.: PolLux: A new facility for soft x-ray spectromicroscopy at the Swiss Light Source, Rev Sci Instrum, 79(11), 113704, doi:10.1063/1.3021472, 2008.

Ransom, B., Kim, D., Kastner, M. and Wainwright, S.: Organic matter preservation on continental slopes: Importance of mineralogy and surface area, Geochim. Cosmochim. Acta, 62(8), 1329–1345, 1998.

Russell, J. D. and Fraser, A. R.: Infrared Methods, in Clay Mineralogy: Spectroscopic and Chemical Determinative Methods, edited by M. J. Wilson, pp. 11–67, Chapman & Hall, London. 1994.

Schlanger, S. O. and Jenkyns, H. C.: Cretaceous oceanic anoxic events: causes and consequences, Geologie en mijnbouw, 55(3-4), 179–184, 1976.

Sherrod, L., Dunn, G., Peterson, G. and Kolberg, R.: Inorganic carbon analysis by modified pressure-calcimeter method, Soil Sci Soc Am J, 66(1), 299–305, 2002.

Sinton, C. and Duncan, R.: Potential links between ocean plateau volcanism and global ocean anoxia at the Cenomanian-Turonian boundary, Econ Geol Bull Soc, 92, 836–842, 1997.

Summerhayes, C. P.: Organic Facies of Middle Cretaceous Black Shales in Deep North Atlantic, AAPG Bulletin, 65(11), 2364–2380, 1981.

Środoń, J.: Quantification of illite and smectite and their layer charges in sandstones and shales from shallow burial depth, Clay Miner., 44(4), 421–434, doi:10.1180/claymin.2009.044.4.421, 2009.

Takashima, R., Nishi, H., Huber, B. T. and Leckie, R. M.: Greenhouse world and the Mesozoic ocean, Oceanography, 19(4), 82–92, 2006.

Theng, B. K. G., Churchman, G. J. and Newman, R. H.: The Occurence of Interlayer Clay-Organic Complexes in Two New Zealand Soils, Soil Sci, 142(5), 262–266, 1986.

Tiller, K. G. and Smith, L. H.: Limitations of EGME Retention to Estimate the Surface-Area of Soils, Aust. J. Soil Res., 28(1), 1–26, 1990.

Tribovillard, N., Algeo, T. J., Lyons, T. and Riboulleau, A.: Trace metals as paleoredox and paleoproductivity proxies: An update, Chem. Geol., 232(1-2), 12–32, doi:10.1016/j.chemgeo.2006.02.012, 2006.

Turgeon, S. C. and Creaser, R. A.: Cretaceous oceanic anoxic event 2 triggered by a massive magmatic episode, Nature, 454(7202), 323–U29, doi:10.1038/nature07076, 2008.

Tyson, R. V.: Sedimentary organic matter: organic facies and palynofacies, Chapman & Hall. 1995.

Tyson, R. V.: The "productivity versus preservation" controversy: cause, flaws, and resolution, in The Deposition of Organic-Carbon-Rich Sediments: Models, Mechanisms, and Consequences, edited by N. B. Harris, pp. 17–33, SEPM Special Publication No. 82. 2005.

van Bentum, E. C., Hetzel, A., Brumsack, H.-J., Forster, A., Reichart, G.-J. and Sinninghe Damsté, J. S.: Reconstruction of water column anoxia in the equatorial Atlantic during the Cenomanian–Turonian oceanic anoxic event using biomarker and trace metal proxies, Palaeogeogr. Palaeoclimatol. Palaeoecol., 280(3-4), 489–498, doi:10.1016/j.palaeo.2009.07.003, 2009.

van Bentum, E. C., Reichart, G. J., Forster, A. and Sinninghe Damsté, J. S.: Latitudinal differences in the amplitude of the OAE-2 carbon isotopic excursion: pCO_2 and paleo productivity, Biogeosciences, 9(2), 717–731, doi:10.5194/bg-9-717-2012, 2012.

Watts, B. and Ade, H.: NEXAFS imaging of synthetic organic materials, Materials Today, 15(4), 148–157, 2012.

Williams, L. B., Canfield, B., Voglesonger, K. M. and Holloway, J. R.: Organic molecules formed in a “primordial womb,” Geology, 33(11), 913–916, doi:10.1103/G21751.1, 2005.

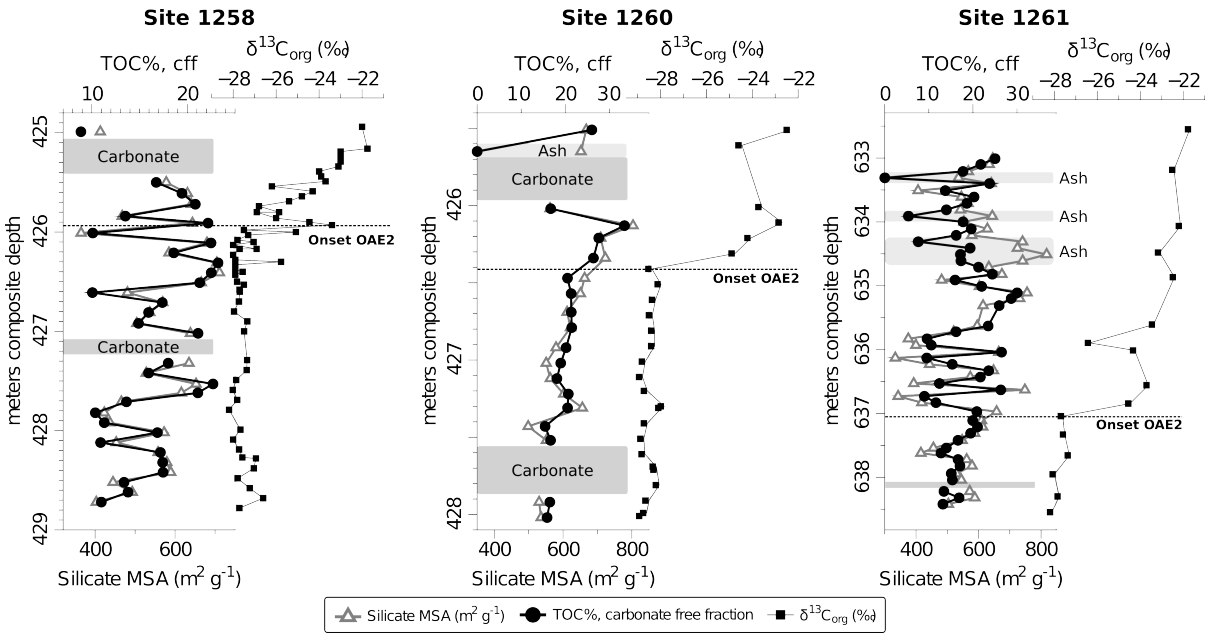

Figure 1. Total organic carbon (TOC) of the carbonate free fraction closely tracks silicate mineral surface area (MSA) in samples from ODP sites 1258, 1260 and 1261, except in ash layers identified in sites 1261 and 1260, where clay mineral formation postdates interaction with organic compounds in the marine and shallow burial environment (Fig. E1). $\delta^{13}C_{org}$ data and interpreted OAE2 boundary are from Erbacher et al. (2005). Samples from carbonate beds (> 85% carbonate) are excluded due to the small detrital component and correspondingly large errors introduced by carbonate correction.

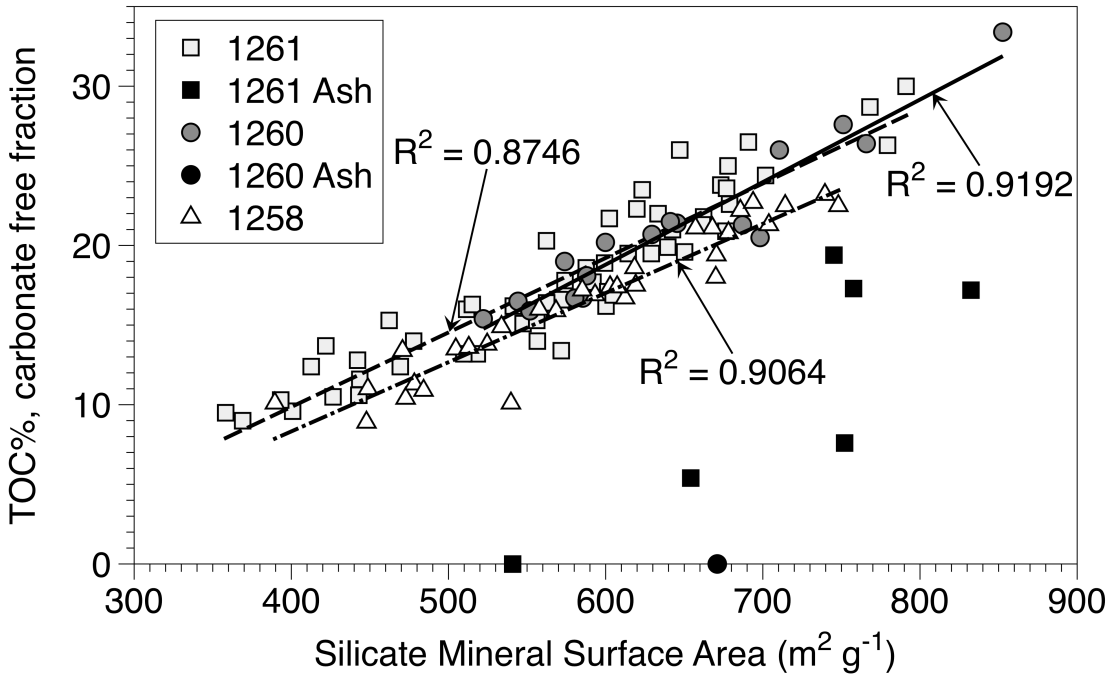

Figure 2. Silicate MSA vs TOC of carbonate free fraction, all sites. Silicate MSA accounts for up to 91.9% of all TOC variation, excluding ash samples (black) and samples with >85% carbonate (not shown). The organic matter in these samples does not contribute to the surface area determined using the EGME method (Fig. 3) and, in any case, if both minerals and OM independently contributed to surface area this would not result in a simple linear regression as shown here.

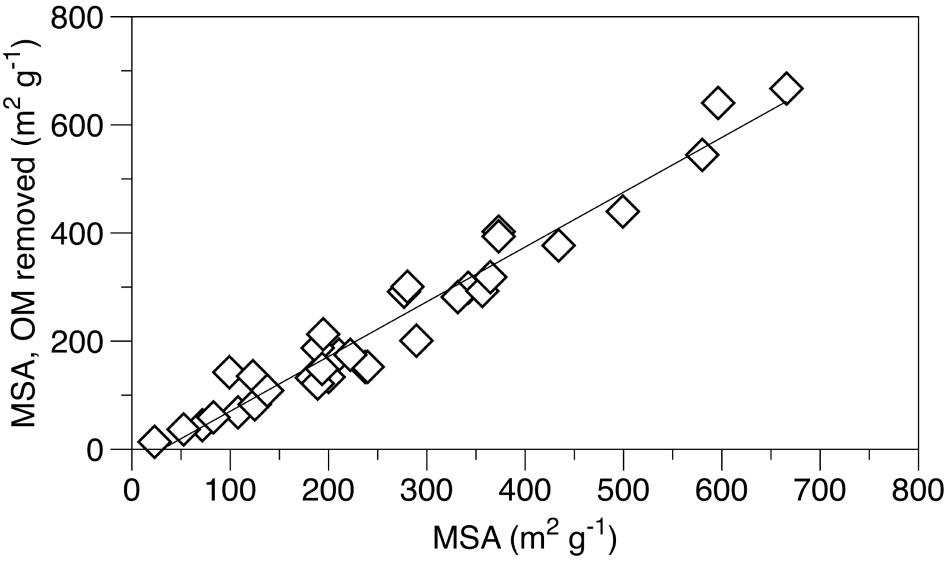

Figure 3. Mineral surface area measured before and after removal of organic matter by H_2O_2 remains essentially unchanged (R^2=0.95), demonstrating that EGME does not interact with organic matter in the samples. Efficiency of OM removal by H_2O_2 ranged between 61–95% (see also supplementary material).

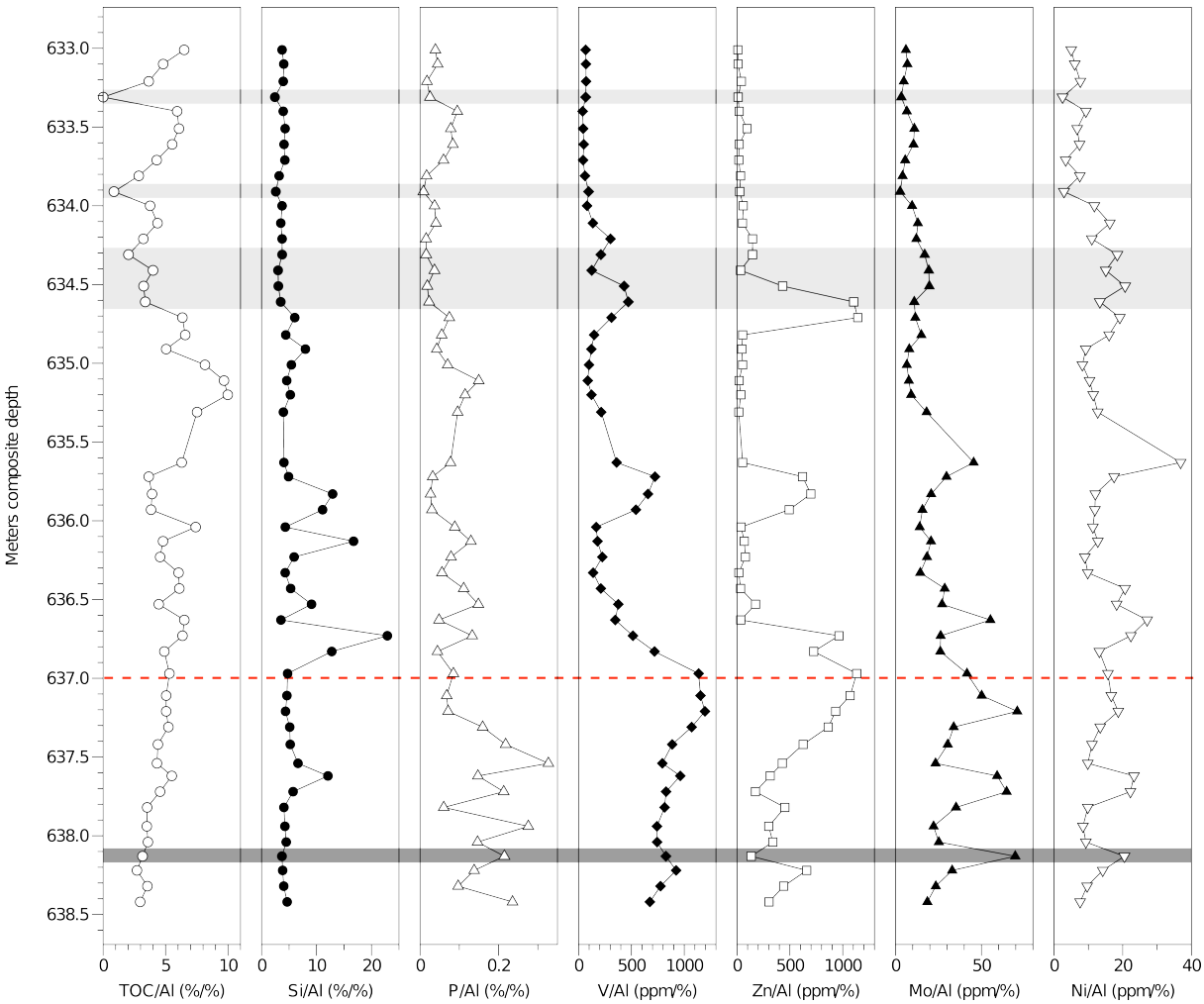

Figure 4. Al-normalised TOC and Si vs redox sensitive elements at Site 1261. Interpreted onset of OAE2 (red) is from Erbacher et al. (2005). Light grey bars denote altered volcanic ash, dark grey zone is a carbonate bed (> 85% $CaCO_3$).

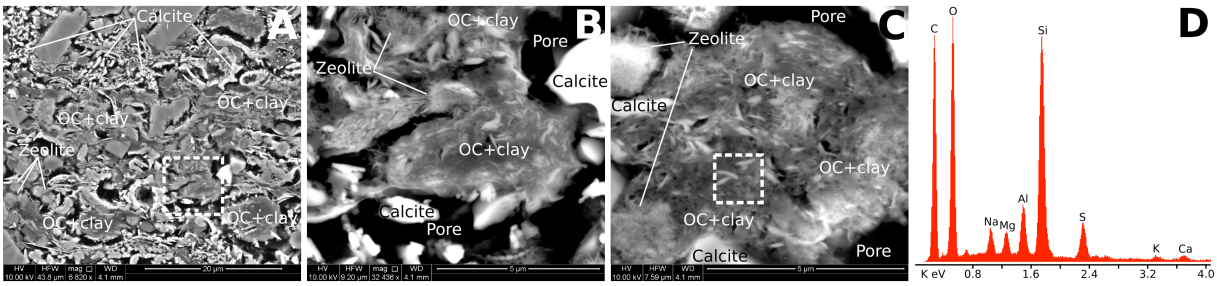

Figure 5. SEM backscatter electron images of Demerara Rise sediments. Organic matter (dark grey in images) is broadly disseminated through the sediment (A) and occurs primarily as sub-µm scale OC coating and aggregated with clays (B+C). Although individual 5-10 µm size aggregates can have the appearance of discrete OM particles (A), closer inspection at higher magnifications (B+C) and energy dispersive X-ray analysis (D, collected from area marked by dashed outline in C) reveals the composite clay-organic nature of these zones.

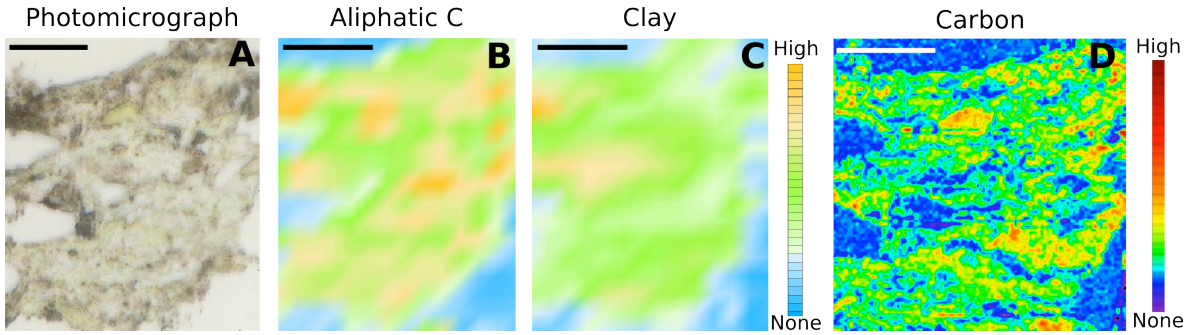

Figure 6. (A) Photomicrograph of 300 nm thick, cryomicrotomed ultrathinsection (Sample 1258/A/43R/3/71-72). (B) FTIR microspectroscopy maps of aliphatic C and (C) clay show broad, overlapping distribution of both over the entire sample (5 µm resolution), consistent with SEM images (Fig. 5). (D) More detailed, higher resolution STXM map of C distribution (25 nm spot resolution, 600 nm step size) in the same sample. Sub-µm scale OC, which is dispersed throughout the sediment (D) in association with clay mineral matrix (C), and is commonly present in organo-clay aggregates (Fig. 5), represents the bulk of OC. Scale bar is 20 µm in all images.

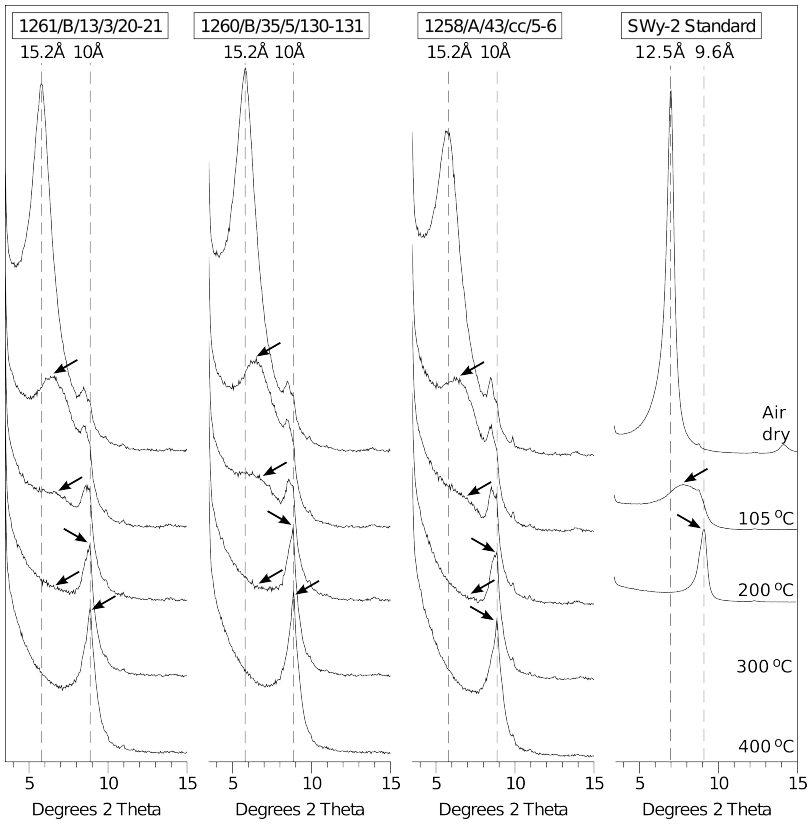

Figure 7. X-ray diffractograms of <2µm fractions of smectite clay standard (SWy-2, Na-saturated) and three representative Demerara Rise samples after air-drying and heating to the indicated temperatures (oriented preparations). Interlayer dehydration in pure smectite (SWy-2) is achieved by heating to >105 °C, and results in complete collapse of the 001 peak to ≈10Å at 200 °C. Demerara Rise samples heated to 105, 200 and 300 °C show incomplete collapse of the 001 peak (arrows mark main peaks and gradual changes), demonstrating the presence of intercalated organic matter that is propping open the smectite interlayer after thermal dehydration has occurred (Theng et al., 1986). Although heating progressively broadens and weakens the 001 peak as it shifts from 15.2 Å towards 13-12Å, representing thermal dehydration, complete collapse resulting in a symmetrical peak at 10Å only occurs after prolonged heating to 400 °C results in thermal oxidation of the intercalated organic matter.